Conceptual Design and Optimization of Small Transitioning UAVs using SUAVE

Emilio Botero*, and Juan J. Alonso†
Stanford University, Stanford, CA 94305, USA

This paper covers the use of SUAVE to analyze, optimize, and design a range of small UAVs. SUAVE has been shown to be a flexible aircraft design tool with the unique ability to handle alternative energy systems. We leverage this ability to use advanced energy networks, add new capabilities for post stall aerodynamics, new mission profiles, vehicle mass models, battery models, and more to design small electric UAVs. In this paper we apply the new methods to existing UAVs, as well as show how SUAVE can be used to design and optimize a family of transitioning UAVs.

Nomenclature

AR	Aspect Ratio	W	Weight
B	Coefficient	b	Wingspan
D	Diameter	c	Chord
$F.S.$	Factor of Safety	k	Coefficient
I	Current, Moment of Inertia	n	Load factor
I_0	No Load Current	t	Thickness
K_v	Speed Constant	t/c	Thickness to Chord Ratio
L	Length	x	Battery State of Charge, Normalized Ordinate
M	Mass	y	Normalized Ordinate
R	Electric Resistance	ρ	Density, Resistivity
S	Wing Reference Area	σ	Stress, Areal Density
$S1$	Lift Curve Slope		
V	Voltage		

I. Introduction

The goal of this work is to allow for the conceptual design of small electric UAVs. The aim is to provide conceptual level simulations of the electronics and vehicle performance that will allow for sizing and optimization. Currently designers often start off with rules of thumb, tricks gained from the design/build/crash test cycle from the radio controlled plane world, or just overpower vehicles to be sure. These strategies begin to break down as the vehicles stray from the tried and true radio controlled configurations.

Additionally, UAVs were traditionally divided into rotor based designs like a quadcopter, and fixed wing designs. Others have developed methodologies into analyzing and optimizing quadrotor types of UAVS.[1,2] We would like to break the boundaries and show that both rotor based UAVs and fixed wing UAVs can be designed together and be analyzed seamlessly with one tool.

The main uncertainties in these designs is the power systems. Designing a power system to meet the thrust requirements of the maneuvering vehicle, while not oversizing the vehicle, compromising payload weight, or payload power available is imperative. One concern for many UAV operators is how the vehicle

*Graduate Student, Department of Aeronautics and Astronautics, AIAA Student Member.
†Professor, Department of Aeronautics and Astronautics, AIAA Associate Fellow.

performs when the battery is pushed to capacity; can the vehicle initiate a go-around or find another spot to land?

This design process becomes far more difficult as we try to create a family of UAVs that range from quadcopters to fixed wing vehicles and in-between using common parts. The constraints become critical, and a designer can no longer 'eyeball it' for 3 or more vehicles.

II. SUAVE Overview

SUAVE is currently a fully functioning aircraft conceptual design tool written in Python. Every major analysis discipline of aircraft design is represented in the code. A full break down of the analysis capabilities of SUAVE are described in prior publications.[3–5] A partial list of the current capabilities is below:

- Aerodynamics for subsonic and supersonic flight,
- Weight correlations for tube-and-wing, blended wing body, and human powered aircraft,
- Segment based mission architecture,
- Static and dynamic stability metrics,
- Propulsion and energy network models including gas turbines, propellers, ducted fans, battery powered, fuel-cell powered, and solar powered vehicles,
- Noise correlations,
- Performance estimation methods such as takeoff and landing field lengths and payload range diagrams,
- Interfaces to optimization packages, that require no changes to the optimization problem setup in SUAVE,
- Geometry output for all supported aircraft configurations through OpenVSP
- High fidelity analyses using CFD through SU2.

The open source nature of SUAVE lends the ability to contribute new analysis capabilities for future aircraft designs. The ability to quickly add new analysis capabilities is critical to this type of work where the next possible technology for UAVs can be quickly experimented with in this fast growing sector.

III. New Capabilities

Several new capabilities were added to SUAVE to handle this type of problem. Prior work showed that large solar UAVs could be optimized with SUAVE, we leverage parts of these capabilities including the propeller, motor, battery, and electronic speed controller analyses. However, these smaller non-solar electric UAVs require different analyses in certain regions of the design space. Here we add in a new aerodynamic model, new mission types, a new voltage model within the battery model, a mass model, and a way to size motors.

A. AERODAS Aerodynamics Model

To model the aerodynamics of the vehicle through transition we require that the aerodynamic model provide results for any possible angle of attack. Through the transition process the vehicle will be stalled at various control points in a segment. Therefore simple linear lift calculations will not work effectively. Aerodynamic coefficients are particularly difficult in determining with separated flow.

Here we introduce the AERODAS model. The AERODAS model is an empirical blend of the pre-stall coefficients of a particular airfoil with a fit for various stalled airfoil sections.[6] This model was originally developed for rotors and wind turbines but has been used in other fixed wing applications.[7,8]

Several deviations from the main technique are made for the inclusion in SUAVE. The main deviation from the model are in the estimation of the maximum lift coefficient for the 2-D section. Here we use existing correlations found within SUAVE. We use the traditional definition of aspect ratio for finite wings,

$\frac{b^2}{S}$, instead of an aspect ratio for rotor blades. Additionally, the slope of the linear region, S1, of the 3-D lift coefficient vs. angle of attack has been replaced with the following:

$$S1 = \frac{S1_p}{1 + \frac{S1_p}{\pi e AR}} \tag{1}$$

Where $S1_p$ is the 2-D lift curve slope in the prestall region. This change is due to the change in definition of aspect ratio. However, the remainder of the methodology is as Spera described.

This only describes how the lift and drag of the wings is calculated. However, it doesn't provide an estimate for drag of the fuselage or any other sources. In this case, we rely on simple calculations using known coefficients that are custom to the vehicle. Depending on the design variables these calculations are scaled in the optimization procedure script to vary with the size as extra drag components.

B. Hover and Transition Segments

Past work with SUAVE looked at airplanes which maybe unconventional in design, but conventional with respect to flight profile. Here we need to expand the mission solving process to work with unconventional mission types. Fortunately, we can leverage much of the same mission architecture in SUAVE that other vehicles use. A list of the new mission segment types are listed below:

- Hover
- Hover Climb
- Hover Descent
- Constant Pitch Rate Constant Altitude
- Constant Acceleration Constant Altitude
- Constant Throttle Constant Altitude

Hover is the most simple segment in SUAVE. Because the vehicle is stationary, aerodynamics effects can be disregarded. Therefore, it is a simple summation of forces between thrust and weight. No ground effect corrections or otherwise are added in the mission.

Two options exist for hover climb and descents. The first is a simple extension of the stationary hover segment with velocities. The second is to use a standard SUAVE climb and descent segment and fix the airspeed to be the same as the climb rate. This makes a vertical climb or descent and includes all aerodynamic forces if applicable.

To model transition we look at three different types of profiles. When looking at transition types we acknowledge that many vehicles perform a parabolic transition where the vehicle pitches forward and loses altitude to ensure the vehicle quickly un-stalls the wings. This is transition type is not smooth and is often done manually. However, we strive to design vehicles which can smoothly go from hover to forward flight. Therefore, the three transitions we look at maintain altitude. The first is a constant acceleration, second a constant rate for tail sitters, finally a constant throttle acceleration.

The constant acceleration profile is simple since the velocities are specified as boundaries and thus all velocities are known throughout the transition. Then the angle of attack and throttle settings are varied and converged to satisfy the force summation.

The opposite is a constant pitch rate, here we know the pitch of the vehicle, and thus the angle of attack. Then the velocities and throttle settings are varied to satisfy the force summation.

Finally, we can set throttle and specify initial and final velocities. Here, the variables are body angle and velocities. The issue with this segment is that it can encumber optimization routines as low throttle segments cannot satisfy the equations of motion.

C. Battery Discharge

A major concern for an operator of a UAV is the power drop at the end of the flight. The voltage profile of a lithium polymer battery tends to be constant around the nominal voltage for much of the capacity. However, there is a tendency for the voltage to drop rapidly towards the end. This voltage drop can be disastrous to the operator as they try to conduct a go-around maneuver from a failed landing attempt. Even though some energy remains in the battery, the voltage drop limits the power that the vehicle can generate. Designing for such conditions means that we must predict the voltage drop and thus modify our designs to allow for go-arounds or know when to stop flying. Rather than arbitrarily setting constraints to final battery capacity, we can set constraints on performance. The performance is really what drives the design.

Chen and Rincon-Mora suggested an exponential fit to this phenomena.[9] To use this we normalize their function to be scaled to order 1. Below is the fit of the battery voltage.

$$V_{normalized} = \frac{-1.031e^{-35x} + 3.685 + 0.2156x - 0.1178x^2 + 0.3201x^3}{4.1} \tag{2}$$

This process requires one to know the charge state of the battery. However, the state of charge affects the voltage. The change in voltage means that the current draw changes, and thus this becomes an iterative process to converge an entire mission. Additionally, we add in the effects of voltage drop due to load.

$$V_{underload} = V_{max}V_{normalized} - IR_{battery} \tag{3}$$

To solve this, we expose the voltage to the mission solver to allow it to be converged. This capability can be enabled or disabled, depending if the user wants to assume a fixed voltage throughout the process. The voltage effect is apparent for these smaller UAVs.

D. Propulsion

Much of the fundamental propulsion modeling for propeller based aircraft in SUAVE still holds to model such vehicles as explained in prior publications.[3] However, a few minor changes were made to improve code speed as well as flexibility. The first change was modifying the propulsor angles such that the orientation and freestream directions are accounted for. The next was developing surrogate models for the propeller. Finally, we developed purely efficiency based motor and propeller models.

By introducing a surrogate model for the existing blade element momentum (BEM) analyses for propellers in SUAVE we can save time but not significantly affect accuracy. This surrogate model interrogates the BEM scripts over a range of predetermined altitudes, velocities, and rotation rates to determine a map for efficiency and the power coefficient. From these we can determine standard outputs such as thrust, torque, and power. This saves computational effort during the mission solution by using the surrogate during the convergence process rather than running the BEM in the loop. The surrogate model primarily leverages the Gaussian Processes available in scikit-learn similarly to what is used in a prior SUAVE publication.[5]

An efficiency based motor and propeller model was also added to SUAVE to enable a lower level of modeling. This kind of capability is important when we focus on sizing a vehicle irrespective of a particular propulsion system based on the assumption of a scalable technology level. This is essential to help size for wing areas when running trade studies between configurations.

E. Vehicle Mass

Determining overall mass of the vehicle is essential to designing such UAVs. Because SUAVE is multifidelity in nature, we have simple correlations as well as a physics based method to determine masses for components. First we will examine the correlation based methods.

1. Mass Correlations

a Structure

To determine the mass of the structural mass of these UASs we begin with correlations. Although SUAVE was intended to be physics based, many pieces and parts of small UASs are not sized to just handle aerodynamic loads typical of large aircraft. Rather these smaller vehicles must be able to withstand handling by operators,

shipping, and rough landings. These loads from these effects can be hard to quantify to feed into more advanced models. For initial sizing these methods are deemed adequate.

Here we introduce correlations by Noth that are fitted to cover over 400 radio controlled models and sailplanes.[10] The function is optimistic in nature as it is fitted to sailplane and glider radio controlled models, but represent a properly designed vehicle.

$$W_{af} = 5.58 S^{1.59} AR^{0.71} \tag{4}$$

This provides the weight of a fixed wing vehicle. Next we must add in the weights of the electronics and any other pieces that enable flight.

b Propeller

To find the mass of propellers a correlation provided by Bershadsky is used.[1] This correlation is a quadratic fit from 30 different propellers including plastic, nylon-plastic, carbon fiber, and wood.

$$m_{propeller} = k_1 D^2 + k_2 D + k_3, g \tag{5}$$

Where the coefficients k correspond to the material type of the propeller shown in Table 1.

Table 1: Propeller Mass Coefficients

	k_1	k_2	k_3
Wood	0.08884	0	0
Plastic	0.05555	0.2216	0
Nylon Reinforced Plastic	0.1178	-0.3887	0
Carbon Fiber	0.1207	-0.5122	0

2. Analytic Sizings

a Wings

This model of the wing is a parametric physics based model. We model the wing as a beam. A major assumption of this type of analysis is that is a solid foam core wing with spar caps. To size the wing mass we consider three different sources. First is the foam core, the second is the spar cap mass, finally we consider the covering.

For a NACA 4 series airfoil we have a thickness function defined as[11]

$$y_t = \frac{t/c}{0.2}(0.29690\sqrt{x} - 0.12600x - 0.35160x^2 + 0.28430x^3 - 0.10150x^4) \tag{6}$$

Integrating we have the following expression:

$$Area_{non-dim} = 2t/c \int_0^1 \frac{1}{0.2} 0.2(0.29690\sqrt{x} - 0.12600x - 0.35160x^2 + 0.28430x^3 - 0.10150x^4)dx \approx \frac{8221t/c}{12000} \tag{7}$$

Finally dimensionalizing and multiplying by span and density for the total mass we have:

$$m_{foam} \approx \frac{8221t/c}{12000} \rho_{foam} b c^2 \tag{8}$$

For the spar caps we use a simplified beam bending theory to size the thickness of the caps. We assume that the width of the spar caps are 5% of the chord length. We assume that the foam core can handle the internal shear stress. The stress from bending for a simple beam is:[12]

$$\sigma = \frac{My}{I} \tag{9}$$

We conservatively assume that the bending moment to be at half of the semi-span leading to:

$$M = M_{TOW}\frac{b}{4}n_{ult}g \tag{10}$$

If we assume a rectangular cross section for the spar caps we can write the moment of inertia of the caps:

$$I = \frac{1}{12}c_{5\%}t^3 + c_{5\%}td^2 \tag{11}$$

Where d is half the maximum thickness of the airfoil section. Given a known maximum allowable stress for the cap material we can solve for the thickness, t in terms of a_1, b_1, c_1:

$$t = \frac{\sqrt[3]{9a_1^2c_1 + \sqrt[3]{3}\sqrt{27a_1^4c_1^2 + 4a_1^3b_1^3}}}{\sqrt[3]{2}3^{2/3}a_1} - \frac{\sqrt[3]{2/3}b_1}{\sqrt[3]{9a_1^2c_1 + \sqrt[3]{3}\sqrt{27a_1^4c_1^2 + 4a_1^3b_1^3}}} \tag{12}$$

where:

$$\begin{aligned} a_1 &= \frac{0.05c_{root}}{12} \\ b_1 &= 0.05C_{root}(\frac{c_{root}t/c}{2})^2 \\ c_1 &= \frac{M(\frac{c_{root}t/c}{2})F.S.}{\sigma_{max}} \end{aligned} \tag{13}$$

Putting the thickness back into solve for the mass of the spar we find:

$$M_{caps} = 2\rho_{spar-material}c_{5\%}bt \tag{14}$$

To estimate the weight of the covering, we numerically integrate over the surface of the airfoil by differentiating equation 6 with respect to x and using it as $\frac{dy}{dx}$ in the following integral:

$$L = \int_0^1 \sqrt{1 + \left(\frac{dy}{dx}\right)^2}dx \tag{15}$$

A clean analytical solution to Equation 15 is not possible, thus numerical integration is necessary. Finally the weight of the covering, where σ is the areal density, is:

$$M_{covering} = 2\sigma_{covering}Sb \tag{16}$$

$$M_{wing} = k_{wing}(M_{caps} + M_{foam} + M_{covering}) \tag{17}$$

b Wiring

An iterative approach is applied in the SUAVE Nexus Procedure script to estimate the wiring mass. Here the designer must have chosen a configuration to determine the characteristic lengths to find the mass of the wiring. The characteristic lengths depend on things such as motor location relative to the battery. If we design in a known voltage drop we can specify wiring with a certain tolerable resistance levels and thus mass.

$$M_{wire} = loss * k_{wire}l^2\rho_{density}V/(I\rho_{resistivity}) \tag{18}$$

c Other Structure

All the remaining structural elements cannot simply be sized using stress constraints from flight loads. Handling requirements as well as available material sizes drive the material thicknesses. In these cases, for parts such as a fuselage, booms for motors, and tail feathers.

To size these we select an areal density for each component. As the vehicle is resized through optimization the wetted areas change, and thus the mass changes with it.

F. Motor Sizing

Current electric motor models in SUAVE rely on data about the motor including the speed constant, no-load current, and resistance. However,these are not entirely independent parameters. Furthermore we seek to know the mass of the motor for vehicle sizing. Here we use correlations by Gur and Rosen to fill the gap.[13] First we start by establishing the coefficients.

$$B_{K_V} = 50(rpm{-}kg/volt) \tag{19}$$

$$B_{R_A} = 60000(rpm^2 - ohm/volt^2) \tag{20}$$

$$I_0 = 0.2(amp - ohm^{0.6}) \tag{21}$$

These coefficients represent the mean of the regressed data. Next we find the mass, resistance, and no load current from speed constant.

$$M_{motor} = \frac{B_{K_V}}{K_V} \tag{22}$$

$$R = \frac{B_{R_A}}{{K_V}^2} \tag{23}$$

$$I_0 = \frac{I_0}{R^{0.6}} \tag{24}$$

Now the motor can be reasonably optimized with speed constant helping define the critical parameters.

IV. Test Cases

We look at current off-the-shelf UAVs of similar sizes to the family we would like to optimize. The first validation case is the DJI S1000+. The second case is a Transition Robotics Quadshot. The intent of the DJI S1000+ validation is to look at the propulsion system modeling. While the Quadshot case illustrates the aerodynamics and vehicle dynamics.

A. DJI S1000+

The DJI S1000+, as shown in Figure 1, is a large capacity octocopter for professional use.[14] This model of octocopter UAV is often used for professional videography. The detailed specifications provided are sufficient to fully define the vehicle in SUAVE. Here we focus on the hover performance, it is provided that the vehicle can hover for 15 minutes at 9.5 kg. The battery is a 6 cell lithium polymer rated at 15000 mAh.

Figure 1: DJI S1000[14]

We make assumptions on the propeller profile given the specifications. The propellers are sized for hover at the power requirements given. The autopilot and on-board electronics have a constant power draw of 20 watts.

The plots in Figure 2 show the difference in voltage while under load as compared to the open circuit voltage. While the power draw to maintain hover is constant, the voltage drop of the battery pack requires the autopilot to increase the throttle setting throughout the flight.

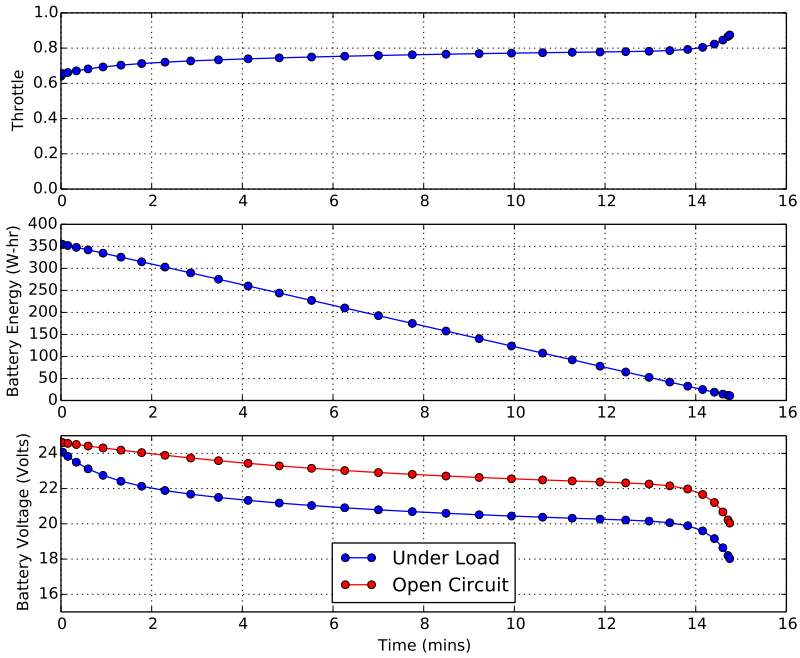

Figure 2: DJI S1000 Power Plots

B. Transition Robotics Quadshot

Next we look to examine the performance and aerodynamics using the Transition Robotics Quadshot. The Quadshot was chosen because of the readily available specifications to model the vehicle in SUAVE as well as the popularity of the design.[15]

In this flight profile we climb vertically, hover, transition to forward flight, cruise for 2 km, transition to hover, hover, then finally descend to land. The altitude, airspeed, and pitch angle throughout this profile can be seen in Figure 3.

This is a rather short mission, however it illustrates all of the pertinent dynamics of a tail sitting UAV. The transitions are modeled as a constant acceleration. For transition to cruise, it is at 1 meter per second. For transition to hover it decelerates at 0.5 meters per second. Interestingly, to decelerate from cruise the vehicle actually pitches back abruptly to stop the vehicle completely. The quickness of the pitch transition shows, how suddenly the vehicle can go from relying on thrust to relying on lift to balance the forces.

Next we look at the aerodynamics of the vehicle, including lift and drag coefficients in Figure 4. We see how the vehicle traverses the drag polar through stall. The maximum coefficient of lift is very briefly reached. Interestingly, the angle of attack on descent is 180 degrees, indicating that SUAVE will generate results both aerodynamic and propulsive results with reversed flow.

V. Optimization Case

In this case we examine the ability for SUAVE to design a family of UAVs. This family has part commonality between a quadcopter variant (QUAD), a purely fixed-wing conventional takeoff and landing variant (CTOL), and a hybrid-configuration vertical takeoff and landing variant (VTOL). The configuration for the VTOL variant is a five motored fixed wing vehicle. Four of the five motors are 'lift' motors while the fifth provides thrust for forward flight. The challenge here is to also design a strictly quadcopter derivative as well as a strictly fixed wing derivative together.

The three vehicles have three separate missions imposed. The QUAD has a hover capability of at least

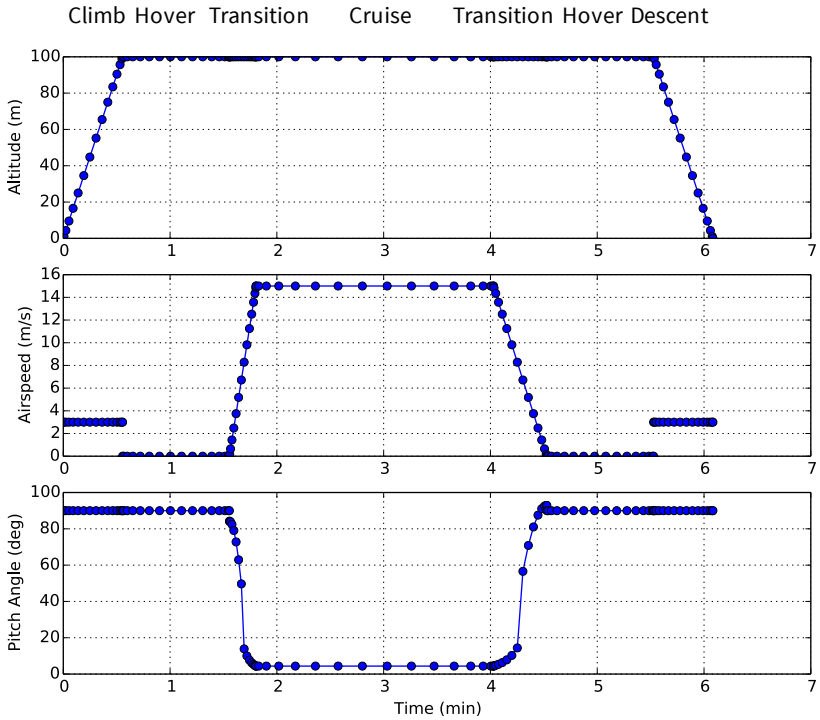

Figure 3: Quadshot Flight Profile

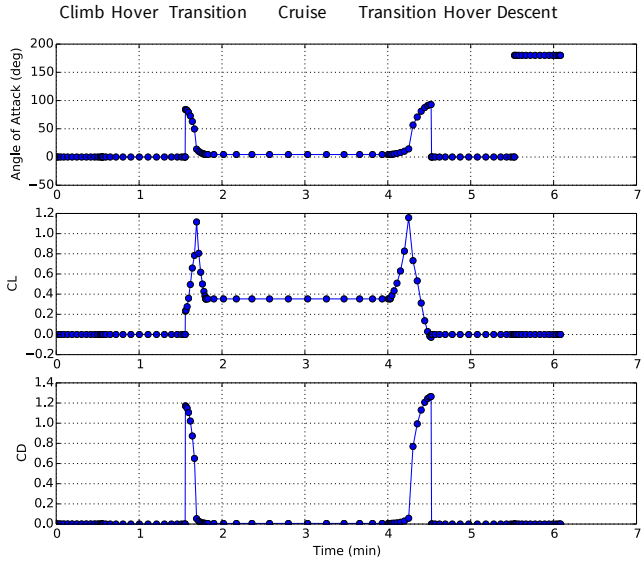

Figure 4: Quadshot Aerodynamic Profile

10 minutes, while the VTOL and CTOL variants can loiter in fixed wing modes for at least 20 minutes and at least 35 minutes respectively. The loiter segments are set to cruise at 20 meters per second. Climbs and descents are modeled. However, the actual transition is not modeled during the optimization process to save computational time. A designer could then use the prior analysis capabilities to determine transition performance.

The payload for this vehicle is a 1U cubesat.[16] The 1U cubesat fixes part of the fuselage dimensions as well as the payload mass and provides an upper bound on power requirements. It also provides some modularity in the final designs to fit a variety of payloads.

The part commonality requires that all 3 vehicles share many critical parts. These common parts include a common fuselage, battery, tail feathers, avionics, payload, motors and propellers as applicable, wiring, and landing gear. Furthermore all components have to be sized to fit the needs of all variants. However, different wings are designed for the two winged variants. This assumption was made to see if the CTOL variant necessitated higher aspect ratio wings, and also provided the ability to attach the lift motors directly to the VTOL variant.

The optimization performed was decided to be simple rather than the detailed models shown earlier. The three variants greatly complicates the analysis, therefore it was decided to use the low fidelity propulsion methodologies described prior. Later analysis and sizing with the higher fidelities within SUAVE can further verify those assumptions. The physics based structural weights outlined earlier are critical here in sizing the vehicle to meet the requirements in this case. Correlations are unlikely to properly estimate the masses in such a complex system of vehicles.

The design variable chosen are listed in Table 2. Less design variables are chosen as the designer deemed many parameters fixed based on physical constraints. For example the propeller diameter was fixed in size, as well as the fuselages. The real key here is sizing the wings for each variant and the other structural members to take the loads of all variants.

Table 2: Design Variables with Bounds

		Lower Bound	**Upper Bound**
Root Chord	[m]	0.1	50
Wing Area, CTOL	$[m^2]$	0.1	50
Wing Area, VTOL	$[m^2]$	0.1	50
Gross Weight, CTOL	[lb]	5.0	55
Gross Weight, VTOL	[lb]	5.0	55

The gross weight, dimensions, required equipment, as well as the payload requirements allow us to calculate the remaining mass which can be used for batteries. The most restrictive battery mass is used for the common family and an energy density of 157 Watt-hours per kilogram are used to calculate the battery capacity for the family based on weighing readily available packaged packs. A six cell lithium polymer battery is assumed. For this battery a cutoff voltage is 3.1 volts per cell.

Table 3 contains the constraints applied to this problem. Some constraints may seem redundant. However, they are necessary. Since the analysis here has a post-stall aerodynamics model a vehicle can be sized which flies at high angles of attack in cruise. However, this differs little from the intent of a multicopter. Similarly, the voltages and energy of the batteries can mislead an optimizer if used alone. Using both was found to be more successful. In this case the constraints are more important to finding a successful design than the objective. The objective in this problem is the takeoff mass of the QUAD variant of the family.

Table 4 shows the results of the above optimization case including the optimal inputs, the satisfied constraints, as well as the final objective. We find that the cruise segment voltage is not an active constraint for the CTOL or VTOL variant. The final mass of the QUAD variant is significantly less than the weight of the CTOL or VTOL version. This indicates that the structural masses of the wings, tails, and the additional motors with propellers drastically alters the weights.

The electronic conditions of the QUAD variant is shown in Figure 5. We notice the linear power drain, but the nonlinear behavior of the voltage drop off.

In Figure 6, we see the simplified mission profile used in optimization. The climb profile is a 15 m/s climb speed with a 4.5 degree climb angle. The cruise velocity is 20 m/s. The altitudes are chosen to starting at

Table 3: Constraints for Optimization Study

Constraints	**Bound**		
Final Voltage, QUAD	$\geq$	18.6	[volts]
Final Voltage, VTOL	$\geq$	18.6	[volts]
Final Voltage, CTOL	$\geq$	18.6	[volts]
Cruise Lift Coefficient, CTOL	$\leq$	0.7	[-]
Cruise Lift Coefficient, VTOL	$\leq$	0.9	[-]
Battery Mass	$>$	0.0	[kg]
Final Battery Energy, QUAD	$>$	0	[joules]
Final Battery Energy, CTOL	$>$	0	[joules]
Final Battery Energy, VTOL	$>$	0	[joules]
Cruise Pitch Angle, CTOL	$\leq$	30	[degrees]
Cruise Pitch Angle, VTOL	$\leq$	30	[degrees]

Table 4: Optimized Family of Aircraft

		Design	Bounds
Root Chord	[m]	0.1	[0.1,50]
Wing Area, CTOL	[m^2]	1.08	[0.1,50]
Wing Area, VTOL	[m^2]	0.97	[0.1, 50]
Gross Weight, CTOL	[lb]	35.7	[5,55]
Gross Weight, VTOL	[lb]	41.3	[5,55]
Final Voltage, QUAD	[volts]	18.6	$\geq$ 18.6
Final Voltage, VTOL	[volts]	19.9	$\geq$ 18.6
Final Voltage, CTOL	[volts]	19.3	$\geq$ 18.6
Cruise Lift Coefficient, CTOL	[-]	0.70	$\leq$ 0.7
Cruise Lift Coefficient, VTOL	[-]	0.90	$\leq$ 0.9
Battery Mass	[kg]	3.43	$>$ 0
Final Battery Energy, QUAD	[joules]	24700	$>$ 0
Final Battery Energy, CTOL	[joules]	47400	$>$ 0
Final Battery Energy, VTOL	[joules]	35300	$>$ 0
Cruise Pitch Angle, CTOL	[degrees]	5.65	$\leq$ 30
Cruise Pitch Angle, VTOL	[degrees]	7.11	$\leq$ 30
QUAD mass	[lb]	21.54	-

5000 feet and ascends to 400 feet AGL. The corresponding aerodynamic conditions are showing in Figure 7. We see the an angle of attack of 10 degrees of approximately and a coefficient of lift of 1.2, which is reasonable for this size aircraft.

Figure 8 shows the mission profile for the VTOL variant. The mission begins and ends with 1 m/s climb and descent. The stalled wing sections contribute to the overall drag during these segments. From Figure 9 we notice the steep slope of the battery discharge during the climb and descent segments. This sharp discharge rate causes the battery voltage to quickly drop during these segments.

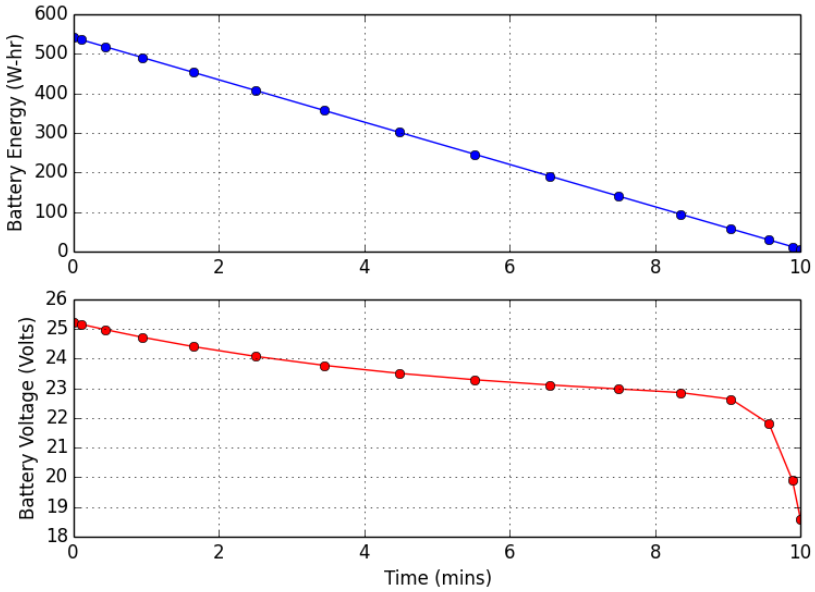

Figure 5: QUAD Electronic Conditions

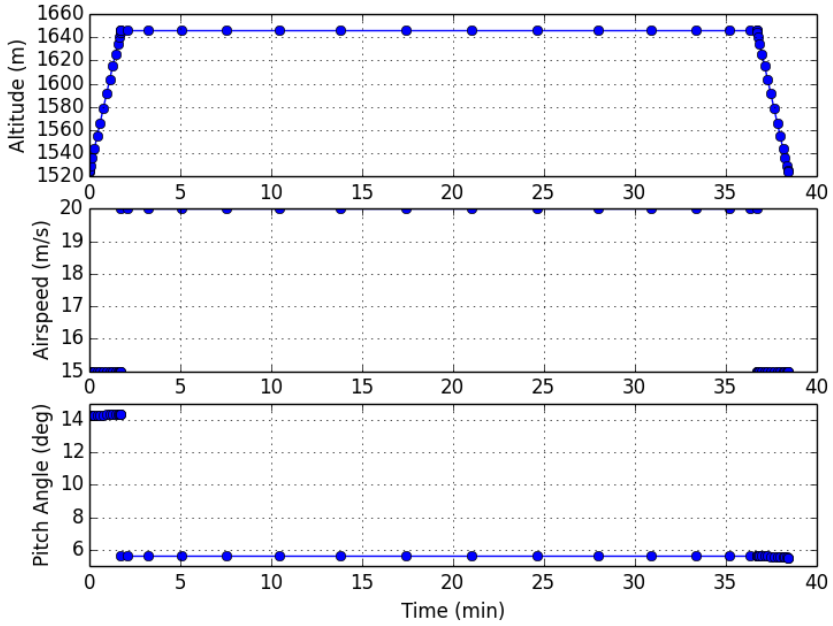

Figure 6: CTOL Mission Conditions

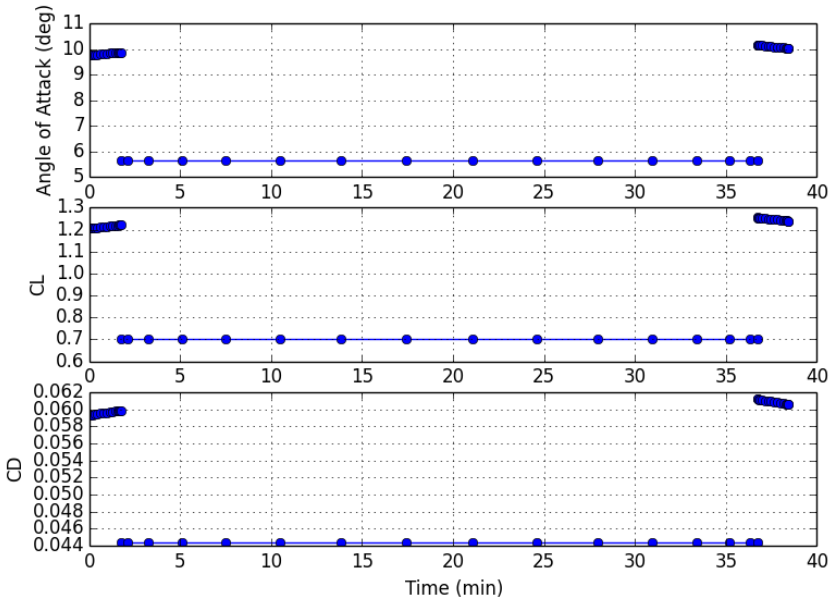

Figure 7: CTOL Aerodynamic Conditions

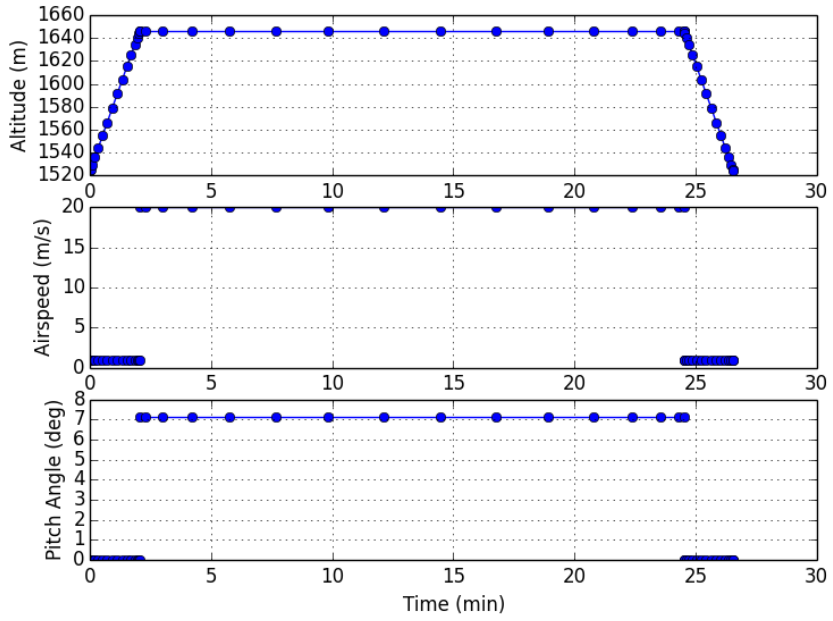

Figure 8: VTOL Mission Conditions

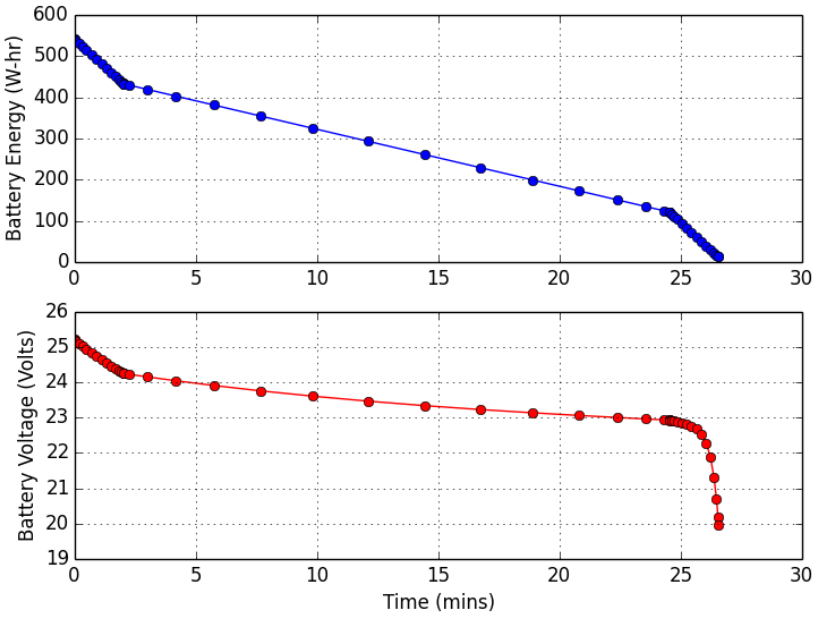

Figure 9: VTOL Electronic Conditions

VI. Summary & Conclusions

We have shown in this paper an approach to UAV design using SUAVE. This methodology is useful for both fixed wing and rotor based UAVs and everything in between. A family of UAVs are designed using part commonality to meet the mission requirements. Many different kinds of UAVs can be designed using these approaches outlined in this work.

New battery models were developed to analyze the voltage drops during flight of UAVs. Parametric structural mass models were created for fixed wing type UAVs that were also applied to a 5 motor transitioning VTOL UAV.

The new battery models were demonstrated using the DJI S1000. The hover times are consistent with the specifications provided by DJI for the S1000. The new mission models and post-stall aerodynamics models were shown on a tail-sitter type vehicle in the Transition Robotics Quadshot.

Finally a family of UAVs were optimized together to show how some of the basic parts of the analysis can be used to create a more complex system of vehicles. This family of UAVs shows how seamlessly one can use SUAVE to analyze both quadcopters and fixed-wing vehicles together.

Future work will research pitching moments during transitions to help size control surfaces and find CG positions. This will be done through incorporating AVL into the current design loop. Furthermore, more research into propeller-airframe interaction is essential to compare configurations. In the above analyses the vehicles have been layout agnostic, only really considering losses of dynamic pressure caused by blockage by forward surfaces. The examples provided here only scratch the surface what SUAVE is capable of analyzing, more exotic designs are up to the reader to conceptualize!

Acknowledgments

Emilio Botero would like to acknowledge the support of the Department of Defense (DoD) through the National Defense Science & Engineering Graduate Fellowship (NDSEG) Program.

References

[1]Bershadsky, D., Haviland, S., and Johnson, E. N., "Electric Multirotor UAV Propulsion System Sizing for Performance Prediction and Design Optimization," *57th AIAA/ASCE/AHS/ASC Structures, Structural Dynamics, and Materials Conference*, 2016, p. 0581.

[2]Winslow, J. M., Hrishikeshavan, V., and Chopra, I., "Design Methodology for Small Scale Unmanned Quadrotors," *55th AIAA Aerospace Sciences Meeting*, 2017, p. 0014.

[3]Lukaczyk, T. W., Wendorff, A. D., Colonno, M., Economon, T. D., and Alonso, J. J., "SUAVE: An Open-Source Environment for Multi-Fidelity Conceptual Vehicle Design," *16th AIAA/ISSMO Multidisciplinary Analysis and Optimization Conference*, AIAA 2015-3087, June 2015.

[4]Botero, E., Wendorff, A. D., MacDonald, T., Variyar, A., Vegh, J. M., Lukaczyk, T., Alonso, J. J., Orra, T. H., and da Silva, C. R. I., "SUAVE: An Open-Source Environment for Conceptual Vehicle Design and Optimization," 2016.

[5]MacDonald, T., Botero, E., Vegh, J. M., Variyar, A., Alonso, J. J., Orra, T. H., and Ilario da Silva, C. R., "SUAVE: An Open-Source Environment Enabling Unconventional Vehicle Designs through Higher Fidelity," *55th AIAA Aerospace Sciences Meeting*, 2017, p. 0234.

[6]Spera, D. A., "Models of lift and drag coefficients of stalled and unstalled airfoils in wind turbines and wind tunnels," 2008.

[7]Ananda, G. K. and Selig, M. S., "Stall/Post-Stall Modeling of the Longitudinal Characteristics of a General Aviation Aircraft," .

[8]Min, S., Harrison, E., Jimenez, H., and Mavris, D., "Development of Aerodynamic Modeling and Calibration Methods for General Aviation Aircraft Performance Analysis-a Survey and Comparison of Models," *Submitted to the 15th AIAA Aviation Technology, Integration, and Operations Conference (AVIATION 2015), Dallas, TX*, 2015, pp. 22–26.

[9]Chen, M. and Rincon-Mora, G. A., "Accurate electrical battery model capable of predicting runtime and IV performance," *IEEE transactions on energy conversion*, Vol. 21, No. 2, 2006, pp. 504–511.

[10]Noth, A., Siegwart, R., and Engel, W., *Design of solar powered airplanes for continuous flight*, Ph.D. thesis, ETH, 2008.

[11]Abbott, I. H. and Von Doenhoff, A. E., *Theory of wing sections, including a summary of airfoil data*, Courier Corporation, 1959.

[12]Sun, C.-T. and Sun, T., *Mechanics of aircraft structures*, J. Wiley, 2006.

[13]Gur, O. and Rosen, A., "Optimizing Electric Propulsion Systems for UAVs," *12th AIAA/ISSMO Multidisciplinary Analysis and Optimization Conference, Victoria, BC, Canada, AIAA Paper*, Vol. 5916, 2008.

[14]"SPREADING WINGS S1000 SPECS," `http://www.dji.com/spreading-wings-s1000-plus/info#specs`, 2016.

[15]"Quadshot Technical Specifications," `http://thequadshot.com/w/index.php?title=quadshot_technical_specifications`, Mar 2013.

[16]Lee, S., Hutputanasin, A., Toorian, A., Lan, W., and Munakata, R., "CubeSat design specification," *The CubeSat Program*, Vol. 8651, 2009, pp. 22.